PCCP

Accepted Manuscript

ROYAL SOCIETY OF CHEMISTRY

www.rsc.org/pccp

The effect of pump-2 laser on Autler-Townes Splitting in Photoelectron Spectra of K_2 molecule

Wei Guo[1*] and Xingqiang Lu[2]

[1]School of Electric Engineering, University of South China, Hengyang 421001, P. R. China.

[2]School of Nuclear Science and Technology, University of South China, Hengyang 421001, P. R. China

Abstract:

We theoretically investigate the Autler-Townes (AT) splitting in the photoelectron spectra of four-level ladder K_2 molecule driven by pump1-pump2-probe pulses via employing the time-dependent wave packet approach. The effect of the pump-2 laser intensity and wavelength on AT splitting is detailed studied for the first time. The triple splitting with asymmetric profiles arises due to the nonresonant excitation. The triple splitting is transformed into double splitting when the pump-2 detuning approached $\pm 1/2$ times of pump-1 Rabi frequency. The splitting between two sideband peaks in the triplet or doublet does not change with the pump-2 laser wavelength. The three peaks shift to lower energy with different shift as pump-2 wavelength increases. The magnitude of AT splitting increases with increasing the pump-2 laser intensity. The asymptotic behaviors of AT splitting with pump-2 laser intensity are interesting in the threshold point of near resonant region and far-off resonant region.

Keywords: Autler-Townes splitting, Photoelectron spectra, four-level ladder K_2 molecule,

PACS number(s): 33.60.+q, 33.20.Xx, 42.50.Hz

* Corresponding author. E-mail: vella99@163.com

1. Introduction

The ac-Stark effect, also known as Autler-Townes (AT) splitting, occurs due to nonlinear interactions between light and matter in the presence of one or more strong variable radiation fields.[1] In recent years, the dependence of AT splitting on laser parameters, such as laser intensity,[6,7,9,12-16,21] pulse width,[4,5,17,19,20] pulse envelope[21] and time delay[2,3] etc. has been studied theoretically and experimentally in multi-level atomic/molecular system of various configurations.

For three-level system, the AT double splitting generally can be observed by using a pump-probe laser configuration, and can be interpreted by the dressed-state theory. Wollenhaupt *et al.*[2,3] observed experimentally the AT double splitting in photoelectron spectra of K atoms, and studied the effect of pump intensity and time delay on AT doublet. They suggested that the asymmetry of the splitting is due to the nonresonant excitation, and the splitting monotonically increases with the laser intensity. Sun and Lou[4] obtained theoretically the AT double splitting in Na_2 molecules, and studied the effect of pump intensity and pulse width on the splitting. The longer pulse can induce the asymmetry of doublet. Yuan *et al.*[5] studied the effects of molecular rotation and alignment on the AT double splitting in Na_2. Yao *et al.*[6] observed the AT double splitting in K_2 molecules, and suggested the pump intensity and wavelength determine the magnitude of splitting and the enhancement of peaks.

Nonlinear effects due to the quantum coherence effect have also been studied in four-level atomic system of various configurations. The AT splitting in four-level system shares some similar features with that in three-level system. Wei *et al.*[7] and Han *et al*[8] studied theoretically the ac Stark effect in a four-level V-type atomic system in the presence of three driving fields. It was found that the absorption spectra can have two or three peaks depending on the intensity and wavelength of the driving fields. The intensity and wavelength of the second driving field has effect on the AT splitting. They used the dressed state theory to explain the absorption peaks in the spectra. Many reports[9-12] studied the AT effect in a strongly driven electromagnetically induced transparency (EIT) resonance with a four-level Λ-type atomic system,. It is found that the absorption spectrum has two or three peaks

structure in general and their positions and relative intensities are affected strongly by the intensities of the driving fields and their detuning. Echaniz *et al.*[13] expected three-peak absorption spectra in four-state N-type atomic system, and studied the trajectories of three peaks as a function of Rabi frequencies and detunings of one couple field. The expectation is verified in a cold Rb sample. Dutta and Mahapatra[14] expected two or three-peaks emission spectra in four-state N-type atomic system, and suggested the double splitting increases with increasing intensity of one couple field. Sandhya[15] studied the absorption profile of a four-level ladder atomic system interacting with three driving fields. It is expected that there is three-peak absorption (dynamic splitting) with strong middle transition coupling. The three-peak splitting is also observed in the absorption profiles in a photonic crystal doped with five-level nanoparticles, they also studied the features of triple splitting with different intensities and/of detuning.[16]

For four-level ladder system, Meier *et al.*[17,18] observed the AT triple splitting in Na_2 molecules driven by three driving fields, and studied the effect of pulse width on the ATsplitting. Longer pulse indicates asymmetric AT triplet. Hu *et al.*[19,20] observed the AT triple splitting in Li_2 molecules driven by three driving fields, and studied the effect of pulse width on the splitting. Longer pulse indicates asymmetric AT triple splitting. Yao and Zheng[21] observed the AT triple splitting with asymmetric profiles in four-level K_2 molecules driven by three driving fields in the near-resonant region, and studied the effect of intensity, wavelength and envelope on the AT splitting when the parameters of the three laser fields change simultaneously, they did not study the case in resonant and far-off resonant region. They also did not study the effect of the parameters of some pump laser field on the AT splitting.

Most experimental and theoretical studies above on the dependence of AT splitting on laser intensity and wavelength are with the four-level N, V, and Λ configuration. Few works are with the ladder configuration. No studies focus on the effect of intensity and wavelength of the second pump pulse on AT splitting in four-level ladder K_2 molecule. This paper presents new data on the nature of the AT splitting in the photoelectron spectra of four-level ladder K_2 molecule driven by pump-1, pump-2

and probe pulses by the time-dependent quantum wave packet method. We discuss the effects of the pump-2 laser intensity and wavelength on AT splitting for three cases: resonant pulse, near resonant pulse, and far-off resonant pulse. The corresponding features are different at different intensities and/or wavelength of pump-2 pulses.

2. Formalism

In this paper, we model the four-level ladder K_2 molecule by four electronic states, ground state $|X\rangle^1\Sigma_g^+$, two excited states $|A\rangle^1\Sigma_u^+$ and $|2\rangle^1\Pi_g^+$, and ionic ground state $|X^+\rangle^2\Sigma_g^+$. For simplicity, they are abbreviated to $|X\rangle$, $|A\rangle$, $|2\rangle$ and $|X^+\rangle$ in order. Fig.1 sketches the potential energy curves of K_2 relevant in this work. A similar model of the K_2 molecule is also employed in experimental[22,23] and theoretical studies.[21,24] In our treatment, we consider the case that pump-1, pump-2 and probe laser fields are simultaneously applied to the K_2 molecule. The molecule in the ground state $|X\rangle$ is resonantly excited to the excited state $|A\rangle$ by pump-1 laser pulse with the central wavelength λ_1 =848nm. The pump-2 laser pulse with the central wavelength λ_2=785nm then excites resonantly the molecule from $|A\rangle$ to $|2\rangle$. Finally, the probe laser pulse with the central wavelength λ_3=785nm is used to detect the emitted photoelectron from the ionization state $|X^+\rangle$. We neglect the rotational degree of freedom in our treatment, since the rotational motion of the heavy K_2 molecules is almost frozen on the femtosecond time scale.

Under the Born-Oppenheimer approximation, the wavefunctions Ψ can be obtained by solving the time-dependent Schrodinger equation

$$i\hbar\frac{\partial}{\partial t}\Psi = H\Psi \qquad (1)$$

The Hamiltonian H of the system can be written as

$$H = H_S + H' = T + V + H', \qquad (2)$$

where $H_S = T + V$ is the Hamiltonian of the K_2 molecule, T is the operator of the kinetic energy of nuclei, V is the potential energy of the system and H' is the interaction between K_2 molecule and laser field. For the four-state model, the wave functions can be written in the column vector

$$\Psi = (\psi_X, \psi_A, \psi_2, \psi_{ion})^T, \tag{3}$$

Where ψ_X, ψ_A, ψ_2 and ψ_{ion} are the wave functions for the ground state $|X\rangle$, excited states $|A\rangle$ and $|2\rangle$, and ionization state $|X^+\rangle$, respectively. The ionization state is a continuum state, and it is discretized into a band of quasicontinuum states in terms of the energies of emitted photoelectron for the numerical calculations. The ionization state ψ_{ion} can be further expressed as

$$\psi_{ion} = \left(\psi^{(1)}, \psi^{(2)}, \ldots, \psi^{(N)}\right)^T, \tag{4}$$

where N is the number of discrete states of K_2 ion.

The kinetic energy T can be expressed as

$$T = -\frac{\hbar^2}{2\mu}\frac{\partial^2}{\partial R^2}\mathrm{T}, \tag{5}$$

Where μ is the reduced mass of the nuclei, R is the distance between the nuclei in K_2 molecule.

$$\mathrm{T} = \begin{pmatrix} 1 & 0 & 0 & \mathrm{o} \\ 0 & 1 & 0 & \mathrm{o} \\ 0 & 0 & 1 & \mathrm{o} \\ \tilde{\mathrm{o}} & \tilde{\mathrm{o}} & \tilde{\mathrm{o}} & \mathrm{I} \end{pmatrix},$$

and $\mathrm{o} = (0, 0, ..., 0)$ is a zero vector with N-component, $\tilde{\mathrm{o}}$ is the transverse of the vector o and I is a $N \times N$ unit matrix.

The potential V can be expressed as

$$V = \begin{pmatrix} V_X & 0 & 0 & \mathrm{o} \\ 0 & V_A & 0 & \mathrm{o} \\ 0 & 0 & V_2 & \mathrm{o} \\ \tilde{\mathrm{o}} & \tilde{\mathrm{o}} & \tilde{\mathrm{o}} & \mathrm{V} \end{pmatrix}, \tag{6}$$

where V_X, V_A and V_2 are the potential curves of the ground state $|X\rangle$, excited states $|A\rangle$ and $|2\rangle$, respectively. And V is a $N\times N$ matrix, which is the discretized states of ionization state $|X^+\rangle$. It can be written as

$$\mathrm{V} = V_X + \mathrm{I} + \begin{pmatrix} \xi^{(1)} & 0 & \cdots & 0 \\ 0 & \xi^{(2)} & \cdots & 0 \\ \vdots & \vdots & \ddots & \vdots \\ 0 & 0 & 0 & \xi^{(N)} \end{pmatrix}, \tag{7}$$

where $\xi^{(i)}$=(i-1) $\Delta\xi$ (i=1,2,…,N)is the energy of the emitted photoelectron.

The interaction H' between K_2 molecule and laser field is given by

$$H' = \begin{pmatrix} 0 & W_{XA} & 0 & o \\ W_{XA} & 0 & W_{A2} & o \\ 0 & W_{XA} & 0 & \mathrm{W}_{2i} \\ \tilde{o} & \tilde{o} & \tilde{\mathrm{W}}_{2i} & \mathrm{O} \end{pmatrix}, \tag{8}$$

where $\tilde{\mathrm{W}}_{2i} = \left(W_{2i}^{(1)}, W_{2i}^{(2)}, ...W_{2i}^{(N)}\right)$ is the vector of coupling between $|2\rangle$ and $|X^+\rangle$ states via laser field with N-component, and O is the $N\times N$ zero matrix. The coupling between two states via external laser field is given as follows

$$\begin{aligned} W_{XA} &= \hbar R_1(R)\cos(\omega_1 t), \\ W_{A2} &= \hbar R_2(R)\cos(\omega_2 t), \\ W_{2i} &= \hbar R_3(R)\cos(\omega_3 t), \end{aligned} \tag{9}$$

Where $R_1 = \frac{1}{\hbar}\mu_{XA}(R)\cdot e_1 f(t)$, $R_2 = \frac{1}{\hbar}\mu_{A2}(R)\cdot e_2 f(t)$ and $R_3 = \frac{1}{\hbar}\mu_{2i}(R)\cdot e_3 f(t)$ are the Rabi frequencies of laser fields for $|X\rangle \to |A\rangle$ states, $|A\rangle \to |2\rangle$ states and $|2\rangle \to |X^+\rangle$ states, respectively. $\mu_{XA}(R)$, $\mu_{A2}(R)$ and $\mu_{2i}(R)$ are the transition dipole moments between different electronic states, e_1, e_2, e_3 are the amplitudes of laser fields, $\omega_1, \omega_2, \omega_3$ are angular frequencies, and $f(t)$ is the envelope which we chose to be a Gaussian function $f(t) = \exp\left[-4\ln 2\cdot(t/\tau)^2\right]$. τ is the full width at half maximum (FWHM) of pulse, is 30 fs in our numerical calculations.

The photoelectron spectrum, as a function of the electronic energy $\xi^{(i)}$, can be obtained as[18,25-27]

$$P\left(\xi^{(i)}\right)=\lim_{t\to\infty}\int dR\left|\psi^{(i)}\left(R,t,\xi^{(i)}\right)\right|^2. \quad (10)$$

The potential energy curves of K_2 molecule employed in our calculations are taken form ref.28-31. These potential curves are in good agreement with relevant spectroscopic constants of experimental results,[32-34] and the detailed information of the potentials can be obtained from ref.35. The transition dipole moments are taken from ref.36 and 37. In this paper, the energies of the emitted photoelectron $\xi^{(i)}$ span over 0-2 eV, and the number of discrete states of the K_2 ion, *N*, equals 120. The time-dependent Schrodinger equation (eq.(1)) is solved by "split-operator Fourier" methods exactly.[37-41] The K_2 molecule is initially populated on its vibrational ground state of $|X\rangle$ state.

3. Results and discussions

Fig.2 shows the photoelectron spectra as a function of the pump-2 laser intensities I_2 at I_1=I_3=4I_0 (I_0=1.0×10^{11} W/cm^2), λ_1=848nm, and $\lambda_2=\lambda_3$=785 nm. The peaks of photoelectron spectra show the triple splitting with symmetric profiles, one central and two sideband peaks. The triple splitting with asymmetric profiles of K_2 molecule has been obtained in the near resonant region of pump-1 with $\lambda_1=\lambda_2=\lambda_3=785\,\text{nm}$. But the resonant case was not studied.[21] The triplet with symmetric profiles has been observed in Na_2 molecule[17,18] and Li_2 molecule.[19,20] This is similar to the expected three-peak absorption (dynamic splitting) in four-level atomic system with various configurations interacting with three driving fields with strong middle transition coupling, i.e. R_2 □ R_1, R_3,[7,8,10,11,13,15] which can be explained in terms of the dressed state formalism. It is also observed in the absorption profiles in a photonic crystal doped with five-level nanoparticles.[16] The splitting pattern of photoelectron spectrum is so-called AT splitting. In terms of the explanation of ac-Stark splitting in dressed state picture, the three-peak structure arises from the sufficient Rabi oscillation within

the resonant region during the ionization process.[4,17-21] From the dressed state theory,[42] the excited state $|2\rangle$ is dressed by the laser field and splits into three substrates, which correspond to the three peaks respectively. From Fig.2, we can see that the magnitude of the triple splitting increases with increasing the laser intensities of pump-2. This is similar to the observation in three-level K,[2,3] Rb,[43] K_2,[6] and Na_2,[4] and four-level K_2.[21] A similar feature is shown in the absorption spectrum for four-level atomic system interacting with three driving fields.[7,8,10-15,44,45] Fig.3 plots the peak positions for the spectra shown in Fig.2 as a function of pump-2 laser intensity I_2 (Fig.3a) and pump-2 Rabi frequencies R_2 (Fig.3b), respectively. The position of the central peak is around 0.474 eV, which simply is $E_{v0}+\sum\hbar\omega_k - V_I(R_0)$,[4,17,19] E_{v0} being the energy of vibrational ground state, $\hbar\omega_k$ the photon energy, and $V_I(R_0)$ the potential of $|X^+\rangle$ state at equilibrium distance R_0 of the neutral ground state, as indicated with arrows in Fig.1. The positions of these three peaks are at $0.474-R/2$, 0.474, $0.474+R/2$ (effective Rabi frequency $R=\sqrt{R_1^2+R_2^2}$ [2,8,10,13,17-21,46]), which correspond to three substates respectively, and this is plotted as a solid line in Fig.3b, which is seen to be in good agreement with the numerical results. It is easily to know the asymptotic behaviors for $R_2 \ll R_1$ and $R_2 \gg R_1$, respectively. When the pump-2 field is weak ($R_2 \ll R_1$), there is a linear splitting proportional to $R_1/2$. On the other hand, with a very large R_2 ($R_2 \gg R_1$), the two side peaks approach a linear splitting proportional to $R_2/2$. These are plotted as dashed straight lines and dotted straight lines in Fig.3b.

Fig.4 demonstrates the photoelectron spectra for different wavelengths of pump-2 (695 nm-895 nm) while keeping the pump-1 resonant, i.e. λ_1=848 nm, at $I_1=I_2=I_3=4I_0$. The pump-2 field detuning is given by $\Delta_2=\omega_2-\omega_{2A}$, ω_{2A} is the frequency of $|A\rangle\rightarrow|2\rangle$ state. When the pump-2 has a zero detuning (i.e. λ_2=785 nm), the spectrum exhibits a triple splitting with symmetric profiles. Asymmetric profiles arise

as the pump-2 is moved off resonance 785 nm. The asymmetry of the splitting is due to the nonresonant excitation. This asymmetry has been observed in double splitting in three-level K atoms[2] and K_2 molecules.[6] A similar feature is shown in the three-peak absorption profiles[45] or emission spectra[14] in four-level atomic system and in five-level atoms.[16] The three peaks move toward the lower energy with increasing the pump-2 wavelengths. This is because that the longer wavelength indicates the lower photon energy, which results lower photoelectron energy. This is identical with the observation in K_2 molecule with Secant pulse and square pulse by Yao and Zheng, but they did not give the results with Gaussian pulse.[21] Fig.5 plots the peak positions for the spectra shown in Fig.4 as a function of pump-2 wavelength λ_2 (Fig.5a) and pump-2 detuning Δ_2 (Fig.5b), respectively. The linear fits are $0.311+0.986\,\Delta_2$, $0.475+0.278\,\Delta_2$, and $0.641+0.981\,\Delta_2$, for peak1, peak2 and peak3, respectively. These indicate that the shifts of the three peaks are different, the two side peaks shift detuning Δ_2, while the central peak shift $1/4*\Delta_2$. This behavior of peaks shift is not shown in earlier works in four-level ladder system. Echaniz *et al.*[13] studied the trajectories of three peaks as a function of detuning of the second couple field with four-level N-type Rb system. Their result indicates the peak shift is not linear to the detuning. Compare Fig.5 with Fig.3, we can see that the splitting between adjacent peaks in the triplet does not equal as that in the resonant case. This is agreement with the fluorescence spectra[9] and absorption spectra[13] in four-level atomic system and in five-level atoms[16] in detuning case of driving field. However, the splitting (0.330eV) between two sideband peaks in the triplet does not change. As the pump-2 is detuned from the resonance wavelength 785 nm, the triple structure is transformed into double structure gradually. This is similar to the evolvement of the absorption spectrum as a function of the second driving field detuning while keeping the first driving field resonant in four-level V-type atomic system interacting with three driving fields.[7] When the pump-2 detuning approached $\pm R_1/2$ (i.e. λ_2=695 nm or 895 nm), there is an anticrossing between the states associated with one of the AT components and

the displaced central component. The doublet formed when the pump-2 detuning approached $\pm R_1/2$ as shown in Fig.4 is best discussed in terms of the doubly dressed states as illustrated in ref.7.

The photoelectron spectrum at the anticrossing region is investigated further as a function of pump-2 laser intensity when the pump-2 detuning Δ_2 equals $R_1/2$, i.e. $\lambda_2 = 715\,\text{nm}$. The result is shown in Fig.6. In the absence of the pump-2 field the spectrum is simply an AT doublet associated with the pump-1 field with two peaks at $\pm R_1/2$. Introducing the pump-2 field causes a doublet splitting in one of these two peaks and results in a three-peak spectrum. This is agreement with the observation in absorption spectra in four-level Λ-type system[12] and susceptibility in three-level Λ-type atom.[47] The peak positions of these three components are plotted in Fig.7 as a function of I_2 (Fig.7a) and R_2 (Fig.7b), respectively, and are again agreement with the prediction of the dressed-state formalism (solid lines in Fig.7b). In particular, when the pump-2 field is weak ($R_2 \ll R_1$), there is a linear splitting proportional to $R_2/\sqrt{2}$ in one of the AT components (see dashed lines in Fig.7b). on the other hand, with a very large R_2 ($R_2 \gg R_1$) the position of the inner component approaches zero detuning (0.637eV), and the two outer components approach a linear splitting proportional to R_2.

Fig.8 shows the influences of the pump-2 wavelength on the photoelectron spectra in the far-off resonant case of pump-2 laser field ($R_2 > R_1/2$). For very large detuning Δ_2, the pump-2 field introduces negligible modification to the probe field response and the dominant feature of the photoelectron spectrum is an AT doublet. Similar to the case in the near resonant region in Fig.4, the two peaks shift to the lower energy with increasing the pump-2 wavelength, due to the longer wavelength indicating the lower photon energy, which results in lower photoelectron energy. Fig.9 plots the peaks positions for the spectra shown in Fig.6 as a function of pump-2 wavelength λ_2 (Fig.9a) and pump-2 detuning Δ_2 (Fig.9b), respectively. From Fig.9,

It is noted that the magnitude of the double splitting does not change with the pump-2 laser wavelength in the far-off resonant case, which is the same as that in the near resonant region. The linear fits are $0.321+0.989\Delta_2$ and $0.650+0.996\Delta_2$ for the two peaks, respectively, indicates that both peaks shift detuning Δ_2.

4. Conclusion and outlook

In this paper, we theoretical investigated the nature of AT splitting in the photoelectron spectra of the four-level ladder K_2 molecule by employing the time-dependent wave packet approach. The observation of photoelectron spectra maps the information on dressed states. We discuss the effects of the laser intensity and wavelength of pump-2 on the AT splitting for three cases: resonant pulse, near resonant pulse, and far-off resonant pulse.

In resonant region, For fixed intensities of pump-1 and probe fields, The photoelectron spectra show the triple splitting with symmetric profiles (in peak height and splitting of two adjacent peaks), and the AT splitting increases with increasing pump-2 intensity. When the pump-2 field is weak ($R_2 \ll R_1$), there is a linear splitting proportional to $R_1/2$. On the other hand, with a very large R_2 ($R_2 \gg R_1$), the two side peaks approach a linear splitting proportional to $R_2/2$.

In the near resonant region, for the fixed intensities of three fields, the photoelectron spectra show the triple splitting with asymmetric profiles (in peak height and splitting of two adjacent peaks), and the splitting (0.330 eV) between two sideband peaks in the triplet does not change with the pump-2 laser wavelength. The peaks shift to lower energy with different shift as pump-2 wavelength increases. Both two side peaks shift pump-2 detuning Δ_2, while the central peak shift $1/4*\Delta_2$. As the pump-2 is detuned from the resonance wavelength 785 nm, the triple structure is transformed into double structure gradually. The doublet formed when the pump-2 detuning Δ_2 approached $\pm R_1/2$ (i.e. λ_2 =695 nm or 895 nm), which is the threshold point of near resonant region and far-off resonant region.

In the threshold point of near resonant region and far-off resonant region, e.g. λ_2=695nm, in the absence of the pump-2 field the spectrum is simply an AT doublet associated with the pump-1 field with two peaks at $\pm R_1/2$. Introducing the pump-2 field causes a doublet splitting in one of these two peaks and results in a three-peak spectrum. When the pump-2 field is weak ($R_2 \ll R_1$), there is a linear splitting proportional to $R_2/\sqrt{2}$ in one of the AT components. on the other hand, with a very large R_2 ($R_2 \gg R_1$) the position of the inner component approaches zero detuning (0.637eV), and the two outer components approach a linear splitting proportional to R_2.

In the far-off resonant region, for the fixed intensities of three fields, the peaks of photoelectron spectra show the double splitting with asymmetric profiles (in peak height), and the splitting (0.330 eV) between the two peaks does not change with increasing the pump-2 laser wavelengths. Both peaks shift to lower energy by pump-2 detuning Δ_2 with increasing pump-2 wavelength.

Acknowledgments

This work was supported by the National Natural Science Foundation of China (Grant No. 41104094, 11174119), the Research Fund for the Doctoral Program of Higher Education, State Eduction Ministry (Grant No. 20114324120002), the Research Foundation of Education Bureau of Hunan Province (Grant No. 12C0370), and the Scientific Research Foundation for the Returned Overseas Chinese Scholars, State Education Ministry.

References

1. S. H. Autler and C. H. Townes. *Phys. Rev.*, 1955, 100, 703.
2. M. Wollenhaupt, A. Assion, O. Bazhan, Ch. Horn, D. Liese, Ch. Sarpe-Tudoran, M. Winter and T. Baumert, *Phys. Rev. A*, 2003, **68**, 015401(R).
3. M.Wollenhaupt, D. Liese, A. Prakelt, C. Sarp-Tudoran, T. Baumert, *Chem. Phys. Lett.*, 2006, **419**, 184.
4. Z. G. Sun and N. Q. Lou, *Phys. Rev. Lett.*, 2003, **91**(2), 023002.
5. K. J. Yuan, Z. G. Sun, S. L. Cong and N. Q. Lou, *Phys. Rev. A*, 2006, **74**, 043421.
6. H. B. Yao and Y. J. Zheng, *Chin. Phys. B*, 2012, **21**(2), 023302.
7. C. J. Wei, D. Suter, A. S. M. Windsor and N. B. Manson, *Phys. Rev. A*, 1998, **58**, 2310.
8. D. A. Han, Y. G. Zeng, W. C. Chen, S. G. Dong, C. Q. Huang, C. Y. Zhu, P. Y. Liang, *Commun. Theor. Phys.*, 2011, **55**, 671.
9. S. M. Sadeghi, J. Meyer and H. Rastegar, *Phys. Rev. A*, 1997, **56**, 3097.
10. L. J. Yang, L. S. Zhang, Z. H. Zhuang, Q. L. Guo, G. S. Fu, *Chin. Phys. B*, 2008, **17**(6), 2147.
11. L. J. Yang, L. S. Zhang, X. L. Li, L. Han, N. B. Manson, D. Suter and C. J. Wei, *Phys. Rev. A*, 2005, **72**, 053801.
12. L. S. Zhang, X. L. Li, J. Wang, L. J. Yang, X. M. Feng, X. W. Li and G. S. Fu, *Acta Phys. Sin.*, 2008, **8**(8), 4921.
13. S. R. de Echaniz, A. D. Greentree, A. V. Durrant, D. M. Segal, J. P. Marangos and J. A. Vaccaro, *Phys. Rev. A*, 2001, **64**, 013812.
14. B. K. Dutta and P. K. Mahapatra, *Phys. Scr.*, 2009, **79**, 065402.
15. S. N. Sandhya, *J. Phys. B*, 2007, **40**, 837.
16. I. Haque and M. R. Singh, *J. Phys.: Condens. Matter*, 2007, **19,** 156229.
17. C. Meier and V. Engel, *Phys. Rev. Lett*, 1994, **73**(24), 3207.
18. C. Meier, V. Engel and U. Manthe, *J. Chem. Phys.*, 1998, **109**, 36.
19. W. H. Hu, K. J. Yuan, Y. C. Han, C. C. Shu, and S. L. Cong, *Chin. Phys. Lett.*, 2007, **24**(6), 1556.
20. W. H. Hu, K. J. Yuan, Y. C. Han, C.C. Shu and S. L. Cong, *Inter. J. Quan. Chem.*,,

2010, **110,** 1224.

21. H. B. Yao and Y. J. Zheng, *Phys. Chem. Chem. Phys.*, 2011, **13**, 8900.
22. C. Nicole, M. A. Bouchene, C. Meier, S. Magnier, E. Schreiber and B. Girard, *J. Chem. Phys*., 1999, **111**, 7857.
23. T. Brixner, G. Krampert, T. Pfeifer, R. Selle and G. Gerber, *Phys. Rev. Lett.*, 2004, **92**(20), 208301.
24. M. Schlesinger, M. Mudrich, F. Stienkemeier and W. T. Strunz, *Chem. Phys. Lett.*, 2010, **490**, 245.
25. E. Charron and A. Suzor-Weiner, *J. Chem. Phys.*, 1998, **108**, 3922.
26. Z. G. Sun and N. Q. Lou, *Phys. Rev. Lett.*, 2003, **91**, 023002.
27. X. Y. Miao, L. Wang and H. S. Song, *Phys. Rev. A*, 2007, 75, 042512.
28. S. Magnier and P. Millie, *Phys. Rev. A*, 1996, **54**, 204.
29. S. Magnier, M. Aubert-Frecon and A. R. Allouche, *J. Chem. Phys.*, 2004, **121**, 1771.
30. A.Jtaij, A. R. Allouche, S. Magnier and M. Aubert-Frecon, *Can. J. Phys.*, 2008, **86**, 1409.
31. A. Jraij, A. R. Allouche, S. Magnier and M. Aubert-Frecon, *J. Chem. Phys.*, 2009, **130**, 244307.
32. M. Broyer, J. Chevaleyre, G. Delacretaz, S. Martin and L. Woste, *Chem. Phys. Lett.*, 1983, **99**, 206.
33. G. Jong, L. Li, T.-J. Whang, W. C. Stwalley, J. A. Coxon, M. Li and A. M. Lyyra, *J. Mol. Spectrosc.*, 1992, **155**, 115.
34. P. Kowalczyck, S. Kasahara, M. H. Kabir and H. Kato, *J. Mol. Spectrosc.*, 2003, **220**, 162.
35. Detailed information on potential energy data is available at http://www-lasim.univ-lyonl.fr/spip.php?rubrique99. In addition, the revelant references can be obtained from this website.
36. R. de Vivie-Riedle, K. Kobe, J. Manz, W. Meyer, B. Reischl, S. Rutz, E. Schreiber and L. Woste, *J. Phys. Chem.*, 1996, **100**, 7789.
37. Q. T. Meng, G. H. Yang, H.L. Sun, K. L. Han and N. Q. Lou, *Phys. Rev. A*, 2003,

67, 063202.

38. D. Kosloff, *J. Phys. Chem.*, 1988, **92**, 2087.
39. T. X. Xie, Y. Zhao, M. Y. Zhao and K. L. Han, *Phys. Chem. Chem. Phys.*, 2003, **5**, 2034.
40. J. Hu, K. L. Han and G. Z. He, *Phys. Rev. Lett.*, 2005, **95**, 123001.
41. T. S. Chu, Y. Zhang and K. L. Han, *Int. Rev. Phys. Chem.*, 2006, **25**, 201.
42. W. T. Hill and C. H. Lee, *Light-Matter Interaction*, Wiley, New York, 2007.
43. Z. J. Du, S. G. Zhang, C. J. Wu, Y. Guan, W. Y Zhao and H. Chang, *Chin. Phys. Lett.*, 2010, **27(10)**, 104202.
44. E. A. Wilson, N. B. Manson and C. Wei, *Phys. Rev. A*, 2005, **72**, 063813.
45. X. L. Li, H. N. Liu and Y. Yang, *Acta Opt. Sin.*, 2011, **31**(1), 0102001(1-1).
46. H. B. Zhang, U. Khadka, J. P. Song, Y. P. Zhang and M. Xiao, EPL, 2011, **93**, 23002.
47. D. A. Cardimona, P. M. Alsing, H. Mozer and C. Rhodes, *Phys. Rev. A*, 2009, **79**, 063817.

Figure captions:

Figure 1. Potential energy curves of K_2 molecule used in the work. The arrows indicate the excitation energy of 1.462 eV (848 nm), 1.579 eV (785 nm), and 1.579 eV (785 nm)respectively.

Figure 2. The photoelectron spectra for various laser intensities of pump-2. The parameters are as follows: I_0=1.0 × 10^{11}W/cm^2, I_1=I_3=4I_0, λ_1 =848nm, λ_2 = λ_3 =785nm, τ =30fs.

Figure 3. Peak positions for the spectra in Fig.2 as function of (a) pump-2 laser intensity I_2 and (b) pump-2 Rabi frequency R_2. Also shown is the result using the dressed-state formalism (curves in solid lines). The dashed straight lines and dotted straight lines indicate the asymptotic behaviors for $R_2 \square R_1$ and $R_2 \square R_1$, respectively. All the other parameters are the same as those in Fig.2.

Figure 4. The photoelectron spectra for various pump-2 laser wavelengths (695nm-895nm) with pump-1 resonant. The parameters are as follows: I_0=1.0×10^{11} W/cm^2, I_1=I_2=I_3=4I_0, λ_1=848nm, λ_3 =785 nm, τ =30fs.

Figure 5. Peak position for the spectra in Fig.4 versus (a) pump-2 laser wavelengths λ_2 and (b) pump-2 detuning Δ_2. Other parameters are the same as those in Fig.4.

Figure 6. The photoelectron spectra for various pump-2 laser intensity with $\Delta_2 = R_1/2$. The parameters are as follows: I_0=1.0×10^{11} W/cm^2, I_1 =I_3=4I_0, λ_1=848nm, λ_2=715 nm λ_3=785 nm, τ =30fs

Figure 7. Peak positions for the spectra in Fig.6 versus (a) pump-2 laser intensity I_2. (b) pump-2 Rabi frequency R_2. Also shown is the result using the dressed-state formalism (curves in solid lines). The dashed straight lines and dotted straight lines indicate the asymptotic behaviors for $R_2 \square R_1$ and $R_2 \square R_1$. All the other parameters are the same as those in Fig.6.

Figure 8. The photoelectron spectra for various pump-2 laser wavelengths

(455nm-695nm) with pump-1 resonant. The parameters are as follows: I_0=1.0×10^{11} W/cm^2, I_1=I_2=I_3=4I_0, λ_1=848nm, λ_3 =785 nm, τ =30fs.

Figure 9. Peak positions for the spectra in Fig.8 versus (a) pump-2 laser wavelengths and (b) pump-2 detuning Δ_2. All the other parameters are the same as those in Fig.8.

Figure 1

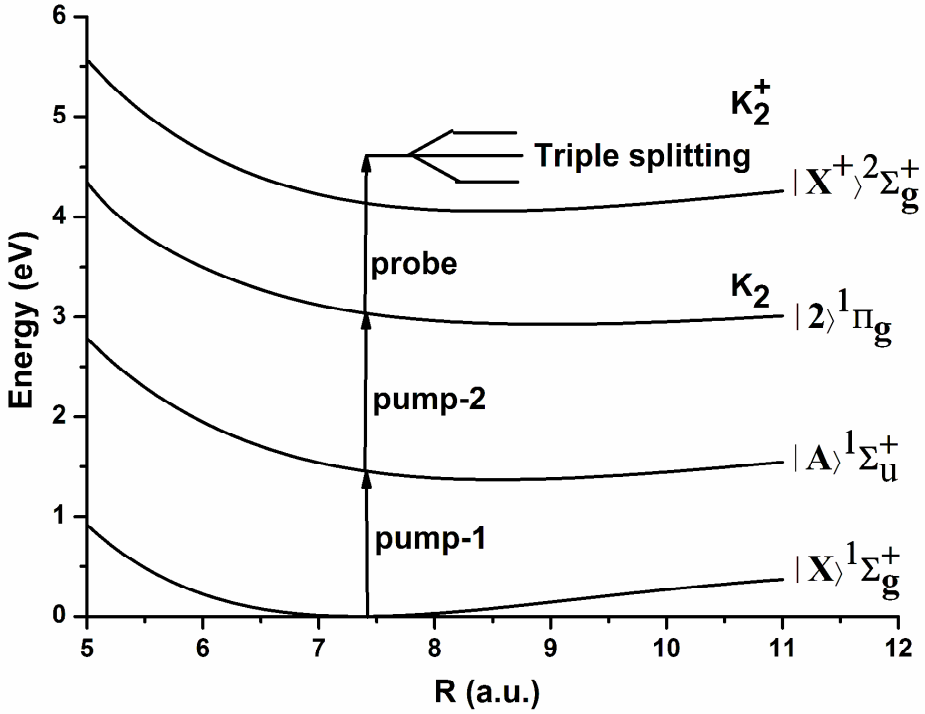

Figure 2

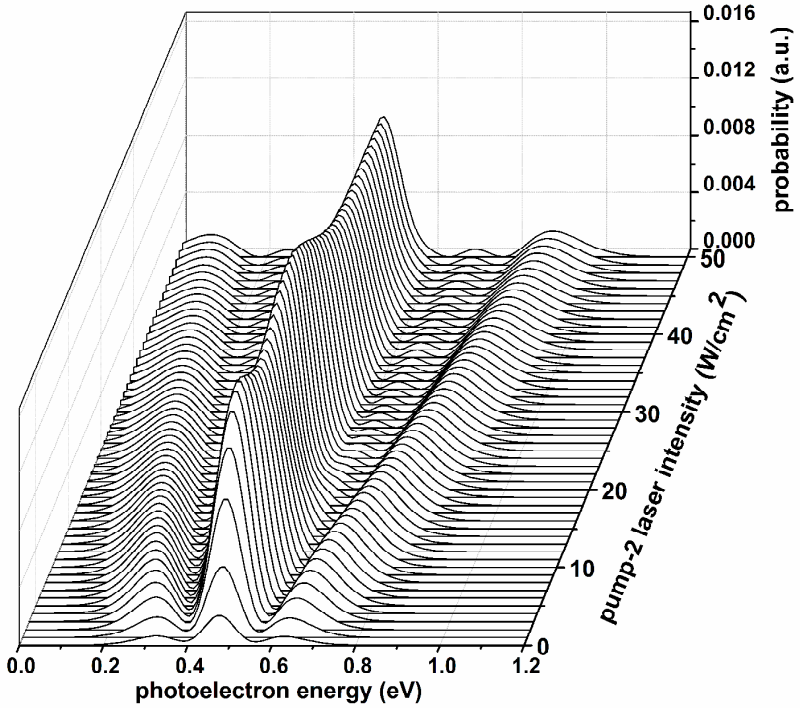

Figure 3

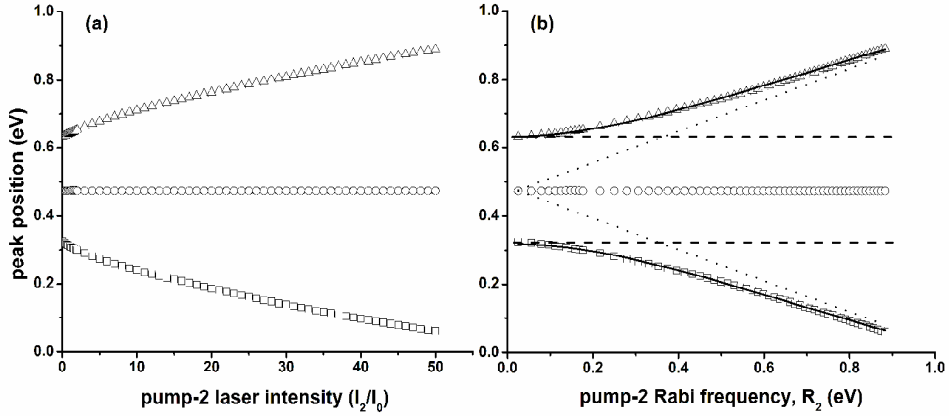

Figure 4

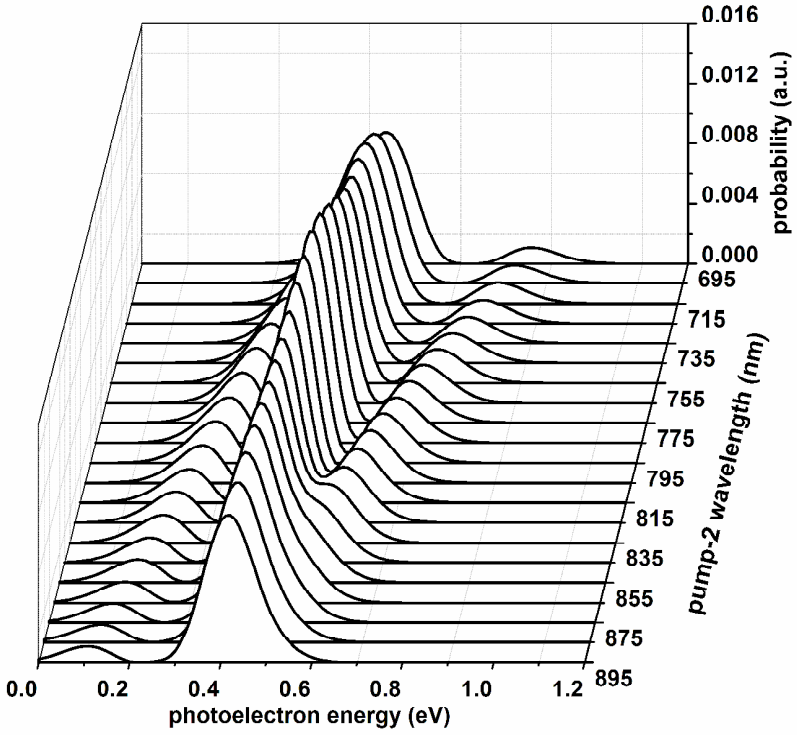

Figure 5

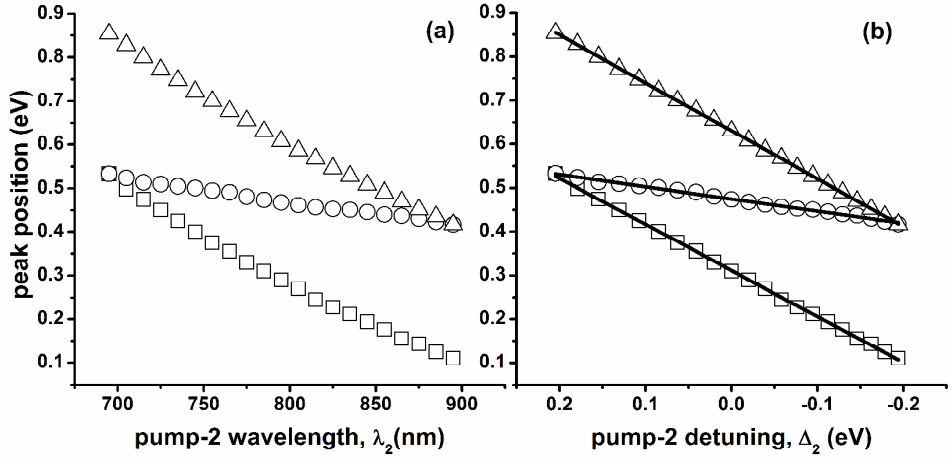

Figure 6

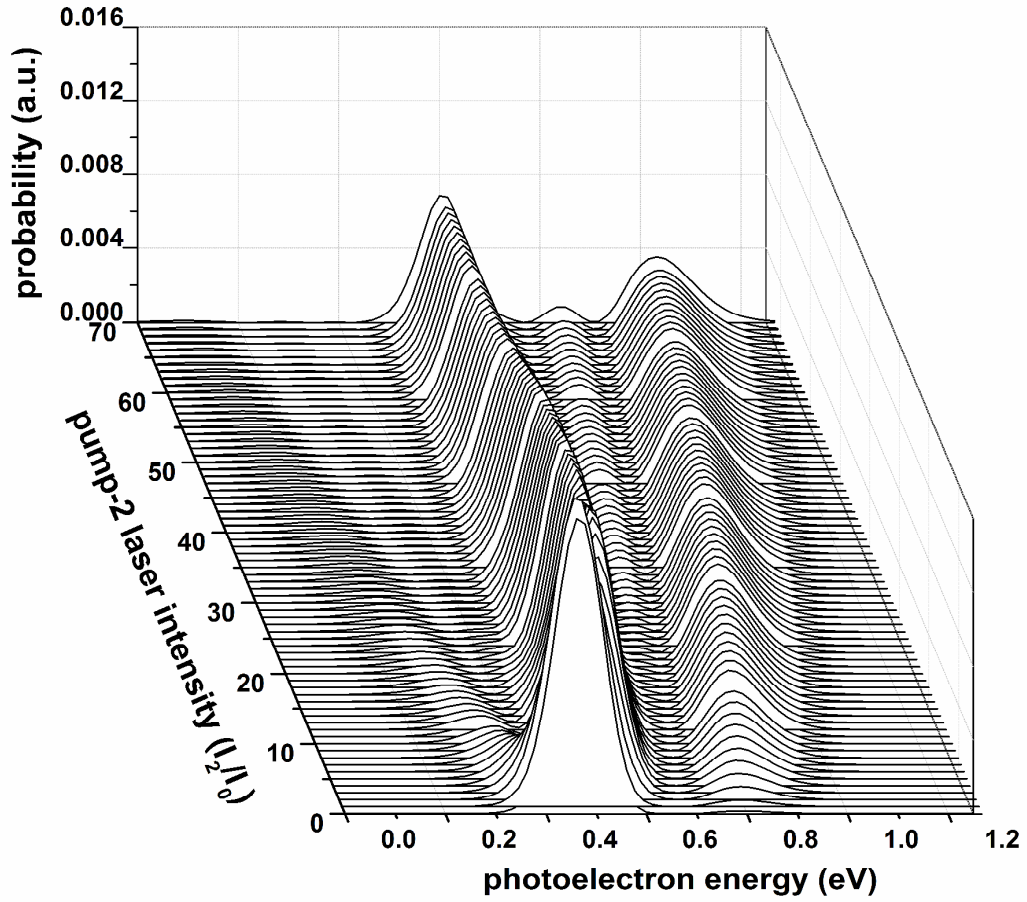

Figure 7

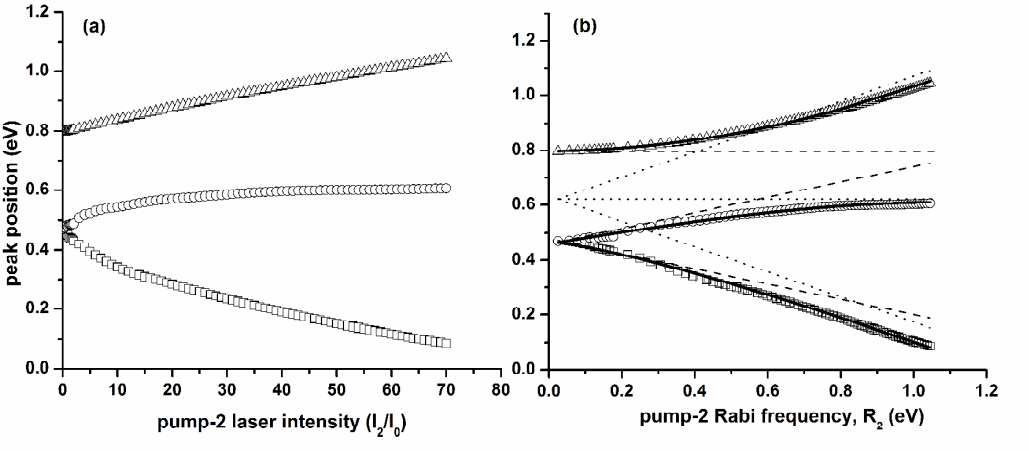

Figure 8

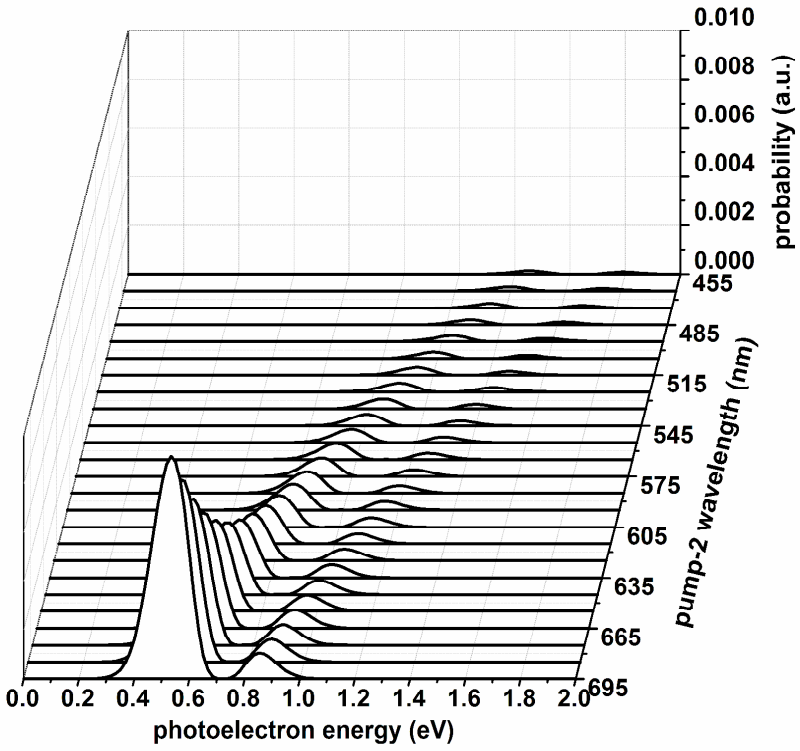

Figure 9

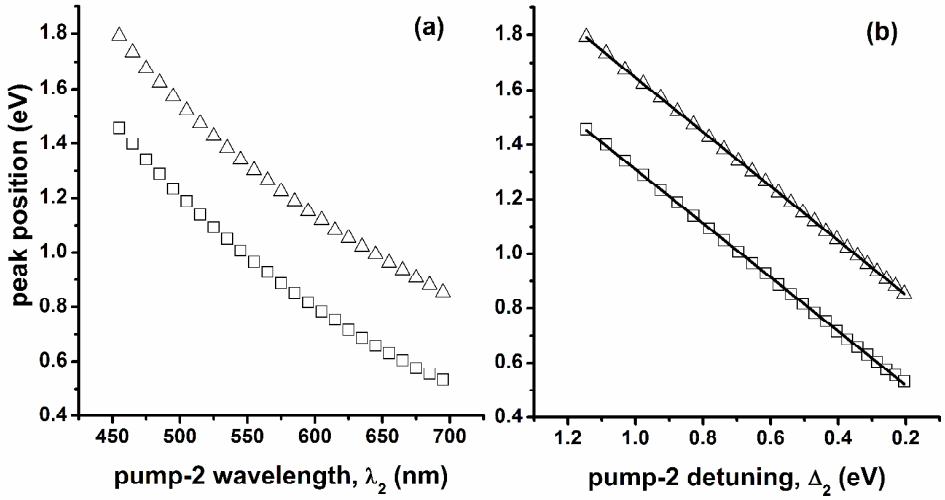

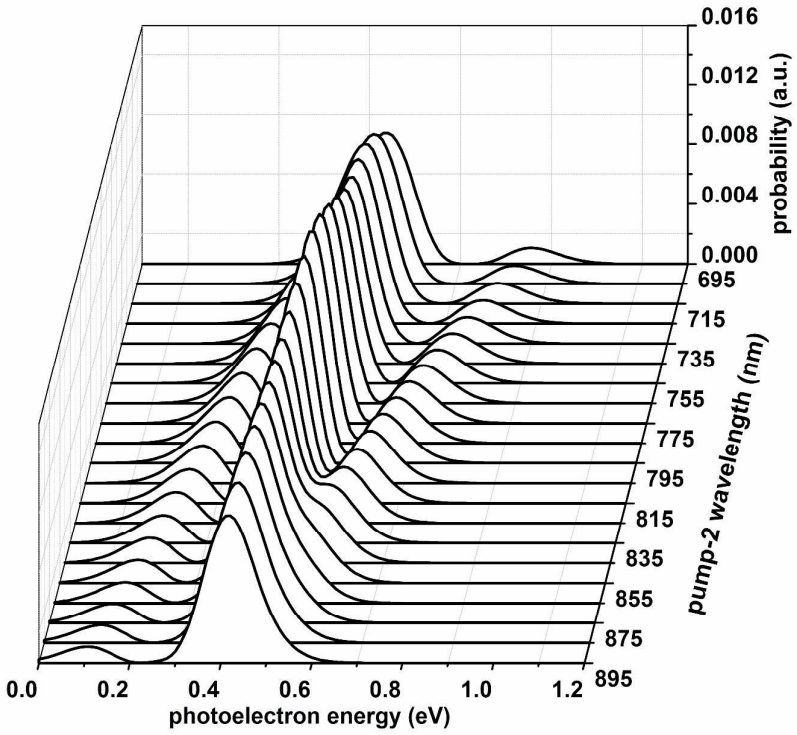

The Autler-Townes (AT) splitting is theoretically investigated in the photoelectron spectra of four-level ladder K_2 molecule driven by pump1-pump2-probe pulses via employing the time-dependent wave packet approach.